Characterisation of 3D printed sand moulds using micro-focus X-ray computed tomography

Tharmalingam Sivarupan and Mohamed El Mansori
Mechanics, Surfaces and Materials Processing, Laboratoire MSMP-EA7350,
Arts et Métiers ParisTech – Centre d'Aix-en-Provence, France, and
Keith Daly, Mark Noel Mavrogordato and Fabrice Pierron
Faculty of Engineering and the Environment, University of Southampton, Southampton, UK

Abstract

Purpose – Micro-focus X-ray computed tomography (CT) can be used to quantitatively evaluate the packing density, pore connectivity and provide the basis for specimen derived simulations of gas permeability of sand mould. This non-destructive experiment or following simulations can be done on any section of any size sand mould just before casting to validate the required properties. This paper aims to describe the challenges of this method and use it to simulate the gas permeability of 3D printed sand moulds for a range of controlling parameters. The permeability simulations are compared against experimental results using traditional measurement techniques. It suggests that a minimum volume of only 700 $\times$ 700 $\times$ 700 μm^3 is required to obtain, a reliable and most representative than the value obtained by the traditional measurement technique, the simulated permeability of a specimen.

Design/methodology/approach – X-ray tomography images were used to reconstruct 3D models to simulate them for gas permeability of the 3D printed sand mould specimens, and the results were compared with the experimental result of the same.

Findings – The influence of printing parameters, especially the re-coater speed, on the pore connectivity of the 3D printed sand mould and related permeability has been identified. Characterisation of these sand moulds using X-ray CT and its suitability, compared to the traditional means, are also studied. While density and 3PB strength are a measure of the quality of the moulds, the pore connectivity from the tomographic images precisely relates to the permeability. The main conclusions of the present study are provided below. A minimum required sample size of 700 $\times$ 700 $\times$ 700 μm^3 is required to provide representative permeability results. This was obtained from sand specimens with an average sand grain size of 140 μm, using the tomographic volume images to define a 3D mesh to run permeability calculations. Z-direction permeability is always lower than that in the X-/Y-directions due to the lower values of X-(120/140 μm) and Y-(101.6 μm) resolutions of the furan droplets. The anisotropic permeability of the 3D printed sand mould is mainly due to, the only adjustable, X-directional resolution of the furan droplets; the Y-directional resolution is a fixed distance, 102.6 μm, between the printhead nozzles and the Z-directional one is usually, 280 μm, twice the size of an average sand grain.A non-destructive and most representative permeability value can be obtained, using the computer simulation, on the reconstructed 3D X-ray tomography images obtained on a specific location of a 3D printed sand mould. This saves time and effort on printing a separate specimen for the traditional test which may not be the most representative to the printed mould.

Originality/value – The experimental result is compared with the computer simulated results.

Keywords Computer simulation, Alloys, Casting, 3D sand mould, Gas permeability, X-ray tomography

Introduction

3D sand mould printing has revolutionised the casting industry – permitting complex shapes to be formed directly from a computer-aided design model within a few days, compared through the traditional pattern making process. Optimisation of the filling and solidification process is made possible through simulation programs, e.g. QuikCAST^{TM}. The significant difficulties for low-pressure sand casting are:

- more accurate implementation of the boundary conditions in the computer simulation before casting; and
- having a mould with the required properties, i.e. a functional mould.

Incorporating this information during simulation permits more efficient use of material, reduced emissions of toxic gases, lower-costs and improved quality casting yeild. A detailed review (Upadhyay *et al.*, 2017) and a few other experimental

The financial support provided by the rapid casting platform, at the MSMP laboratory, of the Low-Cast project is greatly acknowledged. Authors acknowledge the assistance provided by the μ-VIS CT Imaging Centre for the X-ray tomography and the IRIDIS High-Performance Computing Facilities of The University of Southampton, UK. The authors thank Prof Carlos H Caceres, The University of Queensland, for valuable feedback on the final draft. Tharmalingam Sivarupan's current affiliation is School of Mechanical and Mining Engineering, The University of Queensland, Queensland, Australia.

studies (Coniglio *et al.*, 2018; Mitra *et al.*, 2018; Sivarupan *et al.*, 2017) have already been published, by the authors, in relation to the three-point bending (3DP) strength and permeability; hence, this paper contains only a short and concise literature survey. Upadhyay *et al.* (2017) published a review article suggesting the research trend in this field has been increaed due to the possiblility of printing an optimised, complex and large-scale part design by the 3D sand mould printing technology. Coniglio *et al.* (2018) stated that the processing parameters have been influencing the properties of the printed sand mould using a mathematical model. Sivarupan *et al.* (2017) experimentally validated the factors such as recoater speed, print resolution and position in the job-box have greater influence on the properties of the mould; high recoater speed negatively influences the sand packing of the final printed part. Nevertheless, there is still lack of the rules of manufacturing functional 3D printed mould at the industrial level. 3D X-ray computed tomographic imaging of printed sand specimens can improve the information that is used within casting simulations and would help one to analyse the mould properties before casting as this is a non-destructive *in situ* method of identifying the mould properties. In the event of noncompliance with minimum required properties, it can help manufacture a new mould using the proper selection of 3D printing process parameters.

This study aimed to use a geometry obtained from X-ray CT to measure permeability in a virtual environment, ensuring the size, shape and distribution of sand grains are accurately represented in the model. Also, the simulated values were compared with experimental measurements obtained from 3D printed specimens. The sand recoating speed, the speed at which the recoater spreads the sand particles on the job box platform once it has been lowered by a set distance for each printing iteration, was varied and its effect on the pore connectivity and permeability was investigated and incorporated into solidification models – ultimately enabling greater understanding as to how to produce a functional mould for improved casting yield.

Experimental method

Figure 1 shows the spatial repartition of 3D printed sand specimens inside the job box. Sivarupan *et al.* (2017) have stated the experimental result related to the 3PB strength and gas permeability elsewhere and the tomography results are presented here. The CT scan-based imaging can be not just a non-destructive technique but also a method to analyse the actual permeability of any part of the mould; hence, these data can be helpful in simulating the solidification process of an alloy within the 3D printed mould with real/dynamic data (permeability can be a function of time and temperature of the mould) for any size sand mould assembly. A brief explanation of the gas permeabilty measurement procedure is provided in this chapter. The gas permeability tests were carried out using a Simpson® Technologies brand machine to compare with the computer simulated results on the X-ray tomographic 3D model of the sand specimens. The specimens for X-ray computed tomography were printed at the location numbers Z4, Z6 and Z9 (as indicated; on top of the gas permeability test specimens in Figure 1) with the re-coater speed of 0.182 (14 per cent) or 0.286 $mm.s^{-1}$ (22 per cent), and they were all in the Z-orientation. Colour code is provided in Appendix Figure A2.

Coniglio *et al.* (2018), mathematically, and Sivarupan *et al.* (2017), experimentally, identified that the sand recoating speed negatively influences the 3PB (three-point bending) strength and positively affects the gas permeability. This is a follow-up of these two previous studies. The experimental plan is the same as in the previous studies; the first part of the study was on the influence of the printing process parameters on the 3PB response and gas permeability using traditional methods has been published; hence, only X-ray tomography analysis is detailed here, but the results from the previously published articles are used for comparison purposes. An experimental plan (both previous and current), based on the job box in Figure 1, was designed in a commercial software program, NetFabb^{TM}, so that the maximum possible number of samples could be printed in the platform to test the effect of coordinates and other process

Figure 1 Top view of the job-box configurations

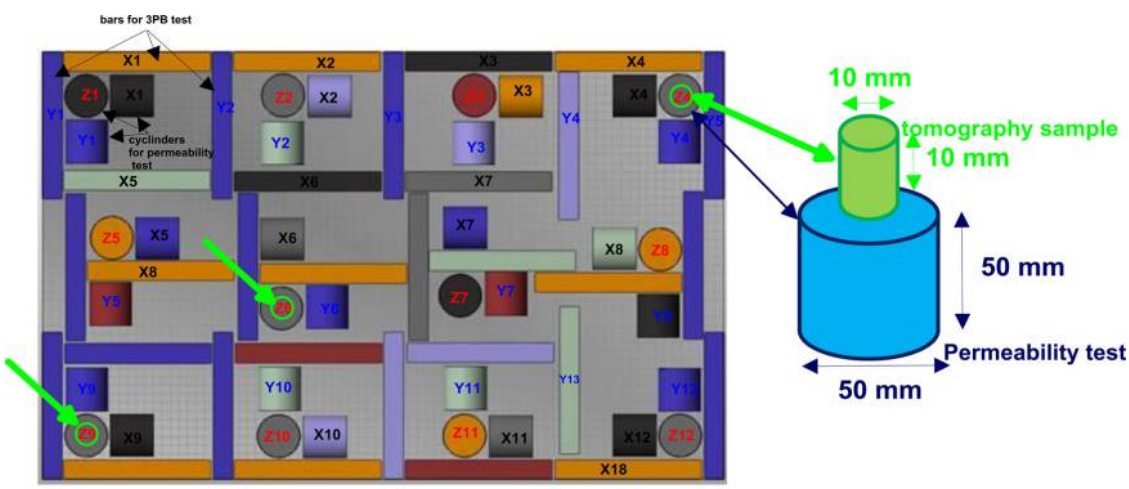

Note: Bars for three-point bending test were in the X- and Y-orientation whereas the cylindrical specimens for the gas permeability test were printed in X-, Y- and Z- directions

parameters (for the previous studies). The results of the prior study are shown in the Appendix Figure A1. Nomenclature of the specimens as per the recoater speed (22 per cent or 14 per cent)-location number (4, 6 or 9), e.g. 22-4, 14-4 or 14-9, see Table I and Figure 1. Only specimens printed at locations Z4, Z6, and Z9, with the following process parameters: activator content (0.18 per cent wt. of sand), mixing time of sand[1] and activator (60 s), and print head voltage (78 V) were all kept constant and the rest according to Table I were used for the present study to understand the compaction of the 3D printed mould using the furan binder[2] – acid activator[3] system using the ExOne S-print 3D sand mould printer (ExOne, 2015). ExOne S-print, located at the MSMP Laboratory of the Arts et Metiers ParisTech, was used to 3D print the sand specimens. It has a job box of 800 × 500 × 400 mm^3 (L*W*H), build speed (voume of sand mould and lose sand in the job-box) of 20000-36000 cm^3/h, adjustable sand layer thickness (Z-resolution) of 0.28 to 0.50 mm, and fixed X/Y resolution of 0.1 mm. The machine can be operated at 400 V, 3-phase/N/PE/50-60 Hz, at a maximum power of 6.2 kW. It can accept the design data input in the form of stereolithography file (STL) as a 2D sliced drawings of the 3D model to be printed.

There were 16 × 3(-*directions*) cylinders[4] to test the permeability and 14 and 18 bars[5] in X- and Y- directions, respectively, to assess the three points bending strength (3PB), in each job-box. The Z-direction by default is weak[6] in 3PB strength and hence not tested. 3PB tests on the printed bars and permeability tests on the cylinders were carried out. The results stated by Sivarupan *et al.* (2017) (see Appendix Figure A1) were compared in the form of a 3D plot to imitate the job box coordinates in the XY plane, and permeability, 3PB strength and density were in the *z*-axis. Only permeability results from the previous study are shown in the Appendix Figure A1 for comparison with the current simulated results on the reconstructed model of the X-ray CT images.

The printing process was begun by mixing the sulphonic acid catalyst with the sand particles, and the mix was stored in the mixing chamber of the 3D printing machine. Then, around ten layers (1.4 mm = five times re-coater movement times two layers each time times the sand particle diameter of 140 μm) of these sand particles were dropped on the job-box before print-head spraying the furfuryl alcohol-based resin on demand as per the first slice of the designed parts (cross-sectional area of the model, stereolithography (STL) file see Figure 1). Then, two layers of these acid-mixed sand particles were spread on the job-box again, once it had been lowered by 280 μm in the Z-direction. The process continued until the last slice of the STL file was printed, and the final two sand layers spread. The specimens were taken out of the job box, cleaned and then tested as stated in the previous paragraph.

The results from a previous study were compared when relevant. The 3D printed specimens obtained at the two extreme sand re-coating speeds[7] of 0.286 (22 per cent) and 0.182 (14 per cent) ms^{-1} were scanned using a micro-focus X-CT system[8] to obtain a 3D model of the actual grain structure, and an electron microscope was used to see the binder distribution. These specimens were only obtained at selected locations of the 3D printer job-box: Z4, Z6 and Z9.

Permeability measurement-traditional (experimental)

The American Foundry Society (AFS) developed a method to measure gas permeability[9] of a sand mould, before the 3D sand printing technology was introduced. It requires a cylindrical specimen with diameter and height of 50 mm and the permeability is measured only along the height of the cylindrical sample according to the equation (1). 3D printed sand specimens show anisotropic properties with the printing parameters such as printing speed, X-/Y-/Z- resolution, and specimen position in the job box. Hence, it is not possible to obtain many cylindrical specimens with various orientations at a specific coordinate in the job box to test and compare the permeability with any other printing parameter. In this situation, there is a vital need for another testing method to obtain permeability of very small 3D printed (<<50 mm) sand specimens. 3D X- CT on a 3D printed small piece of the sand specimen (smaller than 5 mm diameter and height) can be used to simulate the gas permeability in any direction or any other condition, e.g., at various temperature, fluid, specimen size or pressure:

$$G_p = \frac{Q \times h}{F \times p \times t} \tag{1}$$

where G_p is the gas permeability in AFS number[10], Q is the air volume in the chamber (2000 cm^3), h is the height (50 mm), F is the cross-sectional area 19.63 cm^2 of the test specimen, p is the pressure of air in cm of water and t is the time it takes for 2000 cm^3 air to pass through the sample, measured in minutes.

Permeability measurement-simulation (X-CT model)

The X-CT images were acquired using an XT H225 L micro-focus X-CT system (Nikon Metrology, UK). The scans were obtained using a micro-focus 225kV source fitted with a tungsten reflection target together with a Perkin Elmer XRD 1621 detector. The scan settings used were: 100 kV, 83 μA, 354 ms exposure, 3,142 projections acquired during a full 360° rotation using an average of eight frames per projection. No pre-filtration was used other than the beryllium window that

Table I 3D Printing process parameters used in the experiments

Sand recoater speed (Rs) (%)	(mm. s^{-1})	X-resolution of furan droplets (Xr) (μm)	Y-resolution of furan droplets (Yr) (μm)	Z-resolution of furan droplets (Zr) (μm)	Humidity of the room during printing (%)	Temperature of the room during printing (°C)
14	182	120	101.6	280	27	24.6
22	286	140	101.6	280	29	26.2

forms part of the target housing. The specimens were mounted within a custom 3D printed sample holder (Figure 2), enabling six specimens to be installed simultaneously and the scans to be run as an automated batch. Reconstructions were performed using filtered back projection algorithms implemented within CTPro and CTAgent software packages (Nikon Metrolgy, UK), at a 4.8 μm voxel resolution.

Gas permeability modelling

To calculate the permeability, the images had to be converted into a computation mesh on which a series of mathematical problems could be solved. The velocity at which a fluid flows through a permeable medium such as sand is described by Darcy's law, equation (2):

$$\mathbf{v} = -\frac{\mathrm{k}}{\mu}\nabla \mathrm{p}, \tag{2}$$

where $\mathbf{v}$ is the velocity of the fluid, k is the permeability, μ is the viscosity of the fluid and p is the applied pressure. This equation describes a linear relationship between the velocity at which a fluid moves through a medium and the pressure gradient which drives the flow. The constant of proportionality is a combination of the permeability, a property of the porous medium and the viscosity of the fluid, see for example the textbook by Hornung and Springerlink (1997). The permeability can be calculated using the method of homogenisation, see for example the textbook by Pavliotis and Stuart (2008). Briefly, the starting point is the dimensionless Stokes equations for fluid flow, equation (2). A unit pressure drop is applied across a representative sample of the porous material and Stokes' equations are solved to calculate the local velocity. The average velocity can then be calculated and, due to the linearity of Stoke's equations, the permeability can be inferred.

The gas permeability calculation relies on solving equations on a geometry which is assumed to be representative of the porous medium. If the geometry used is too small, then the result will be inaccurate. For example, if the geometry considered was significantly smaller than a grain of sand then a randomly chosen element of geometry may only capture sand or pore space. In this case, the effective permeability would be either zero or infinite. Alternatively, if the geometry is too large, then the simulation time will become prohibitive. Hence, the permeability is calculated for samples of increasing sizes until the results converge. This provides a representative permeability value and an estimate of the size of geometry which is representative of this problem.

Figure 2 Photograph showing specimens contained within a custom 3D printed holder to enable batch scanning of all six specimens

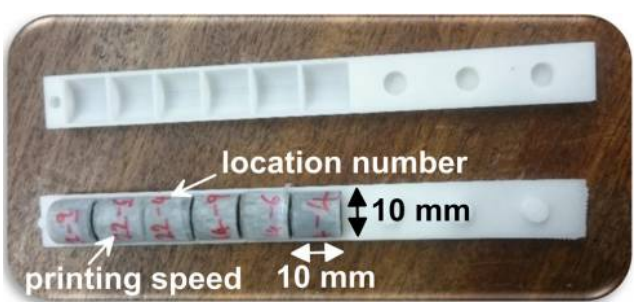

To generate the geometry, on which the equations were solved, first, a threshold was applied to the greyscale volume images. This threshold determined which grey levels in the CT images correspond to pore space and which correspond to sand grains. A default thresholding algorithm was used in ImageJ software package. This was an implementation of the iterative means algorithm which uses iteration to ensure the threshold value was halfway between the average greyscale values above and below the threshold. A surface mesh was then generated based on the thresholded image which represents the 3D sand surface. The mesh was generated using scanIP, a commercial software package.

The surface mesh was used to generate a computational mesh on which Stokes' equations could be discretised and solved. The mesh generation and solution were achieved using the snappyHexMesh package, part of the OpenFOAM distribution. OpenFOAM is an open source CFD package (Jasak *et al.*, 2007) which is based on the volume of fluid method for solving the Navier–Stokes equations.

The geometries considered had side lengths from 125 to 2000 μm (from less than 1 sand grain to around 14). The permeability was calculated in each of the x, y and z directions for each of the imaged samples. Once discretised, the equations were solved on a supercomputer. The largest simulations ran on four 16-core nodes, each with 64 GB of memory.

Results

The simulated (on X-CT model of the 3D printed sand specimens) and experimental gas permeability values were plotted, Figures 3-5 and Figure A1, to compare the effect of recoater speed and/or the printing resolution on the sand packing, for various sample sizes (only for simulated).

Simulated permeability values in the Z direction for all specimens were lower than that in the X or Y direction for a particular recoater speed during printing, Figure 3; the simulated results represent the averaged permeability value obtained when the specimen size is greater than 700 mm side length. Refer to Figure 1 for the position number of the printed specimens. The simulated results seem to converge with increasing sample size and stabilise beyond the sample size with a side length of 700 μm, Figures 4-5. The calculated average[11] permeability values were 37.84×10^{-7} cm^2, 39.54×10^{-7} cm^2 and 34.94×10^{-7} cm^2 in the X, Y, Z directions, respectively, for a recoater speed of 182 mm.s^{-1} (14 per cent); the corresponding values for a recoater speed of 286 mm.s^{-1} (22 per cent) were 61.8×10^{-7} cm^2, 61.94×10^{-7} cm^2 and 55.65×10^{-7} cm^2, respectively. These average values were calculated for a specimen side length greater than 700 μm as this appears to be the minimum side length for consistent simulation results. The trend in the permeability values directly depends on the cross-sectional resolution of furan droplets printed perpendicular to the test/gas flow direction; Figures 3 and 5(d) illustrates this trend. Density, pore volume fraction, minimum permeability obtained from simulation and other relevant data are summarised in Table II. Sivarupan *et al.* (2017) previously published a part of this experimental result elsewhere and the obtained experimental results are

Figure 3 The normalised data (between the minimum and maximum) of the permeability values obtained by simulating (x, y and z directions) it on the reconstructed X-ray tomography specimens, and the normalised experimental (only z-direction) results, on the 3D printed sand specimens when Rs = 0.182 and 0.286 ms^{-1}

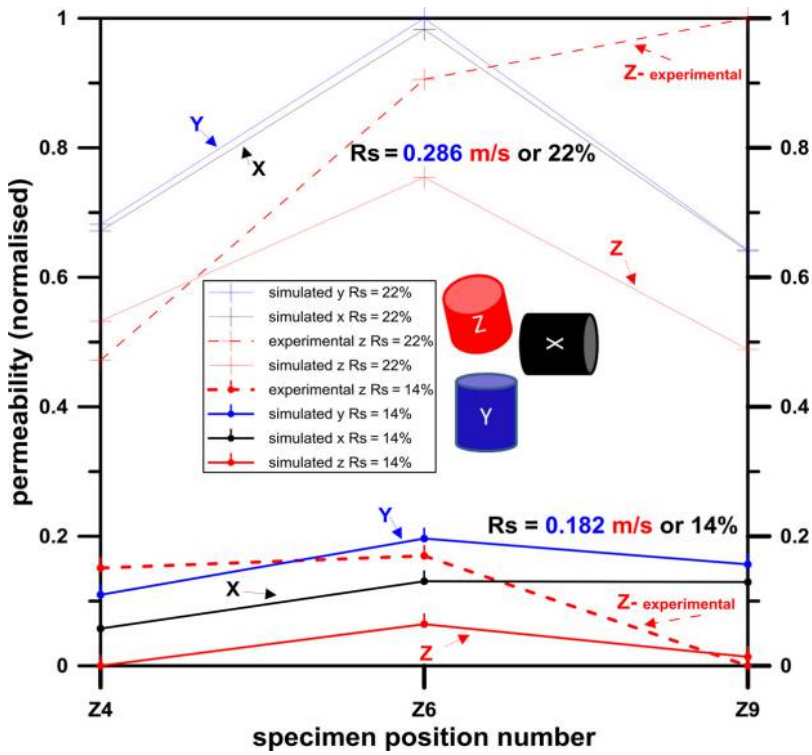

summarised in the Appendix Figure A1 only for qualitative comparison with the current simulated permeability values as the experimental and simulated permeability followed different methods. It shows that at a critical speed of recoater, the permeability values seem to reduce the variation along the job box coordinates; the critical speed was identified as 0.182 ms^{-1} (14 per cent).

Electron microscope images, Figure 6(a-c), on the 3D printed sand moulds (the resin-bonded silica sand[12]) revealed that the specimen printed with the recoater speed of 0.286 (22 per cent) $m.s^{-1}$ showed internal cracks on the furan bridges between the sand grains, compared to the other specimens. X-ray tomography slice, Figure 6(d), shows that there are non-uniform packing of sand particles (bright region) and larger pore (dark region) regions. The reconstructed pore model from the X-ray tomography slices for all of the specimens are presented in Figure 7 and the computed volume fraction and other data are presented in Table II. Experimental density values are added in the corresponding column for reference in Table II. Other process parameters used in the experiments, activator content (0.18 Wt.% of sand), mixing time of sand[13] and activator (60 s) and print head voltage (78 V), were all kept constant. The gas permeability is expressed in AFS number for the experimental results (traditional method for sand mould) and the simulated permeability is in the standard SI unit, but they follow entirely different ways of calculation even though the trend can be compared here with the recoater speed, see Figures 3-5. The pore volume fraction mainly depends on the speed of recoater, Table II and Figure 7. Higher recoater speed leads to poor sand packing.

Discussion

One of the challenges in general sand casting is the lack of proper non-destructive characterisation of the local density of the Figure 8 mould. The CT technique is a promising method to allow non-destructive and contact-free visualisation and characterisation of internal volume and the external surface of a sand mould, including those 3D printed. The primary issue with the 3D printing is the anisotropic sand compaction, and this plays an essential role in the quality of the mould and hence of the quality of the manufactured casting. The permeability of the ExOne 3D printed sand mould can be significantly decreased by increasing curing temperature, without considerable change in the 3PB strength upto 100°C allowing longterm storage of the mould before its use. Mitra *et al.* (2018) The same was previously investigated on the ZCorp printed specimens, which identified the optimum curing time and temperature (Mckenna *et al.*, 2008), position and orientation of printing (FRASCATI, 2007) for the strength and permeability of ZCorp specimens. However, the ExOne printed specimens does not necessarily require curing due to the self-curing polymerization but a proper heat treatment of the mould can be implemented to remove the byproduct from the polymerisation of the furfurylyalchohol based monomers (the resin), the water, from the mould and hence result in

Figure 4 Results from the image-based simulation for the sand permeability

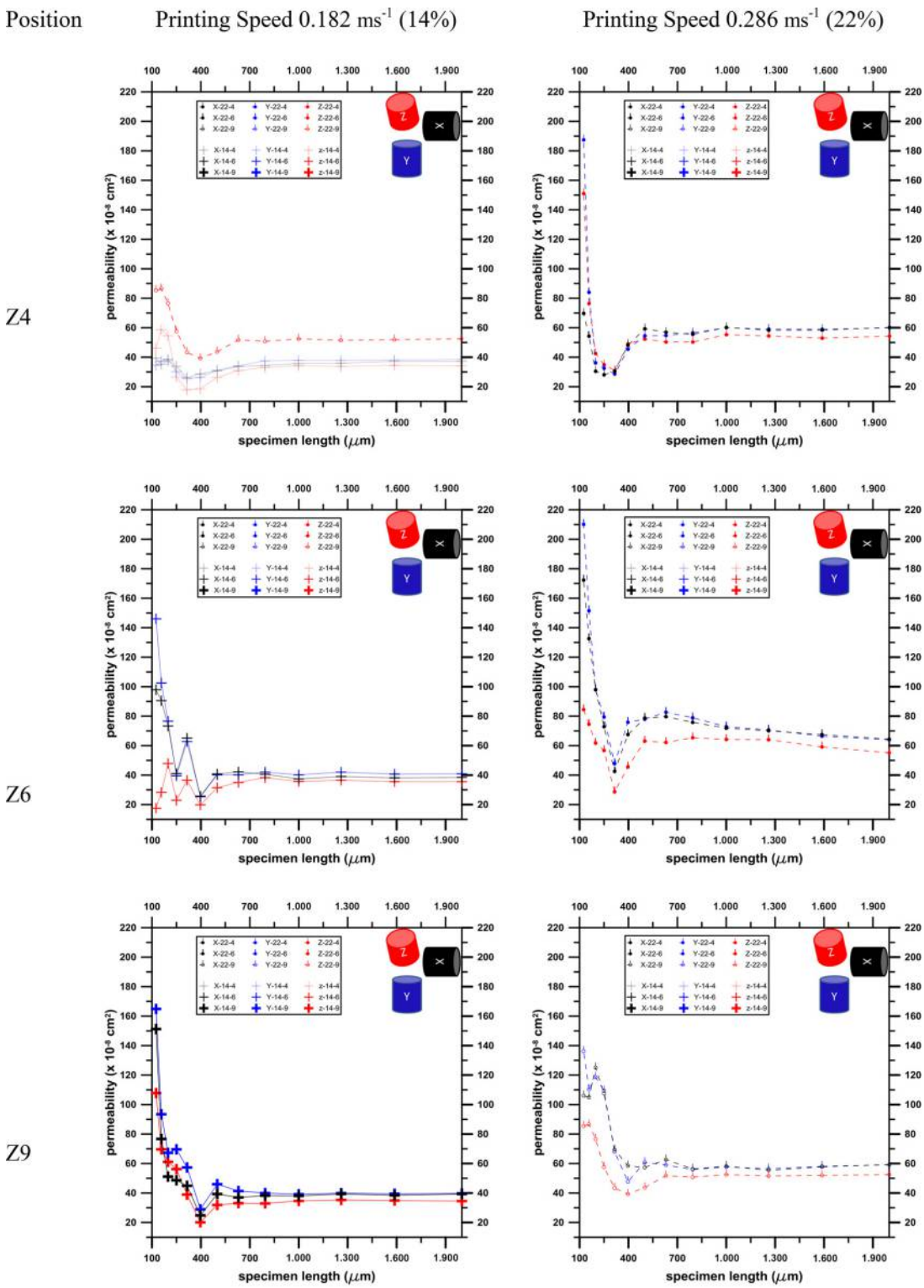

Note: Results are shown in the x, y and z directions for each of the six samples, for the speed and locations as indicated on the top and side of the figures

Figure 5 Results from the image-based simulation for the sand permeability

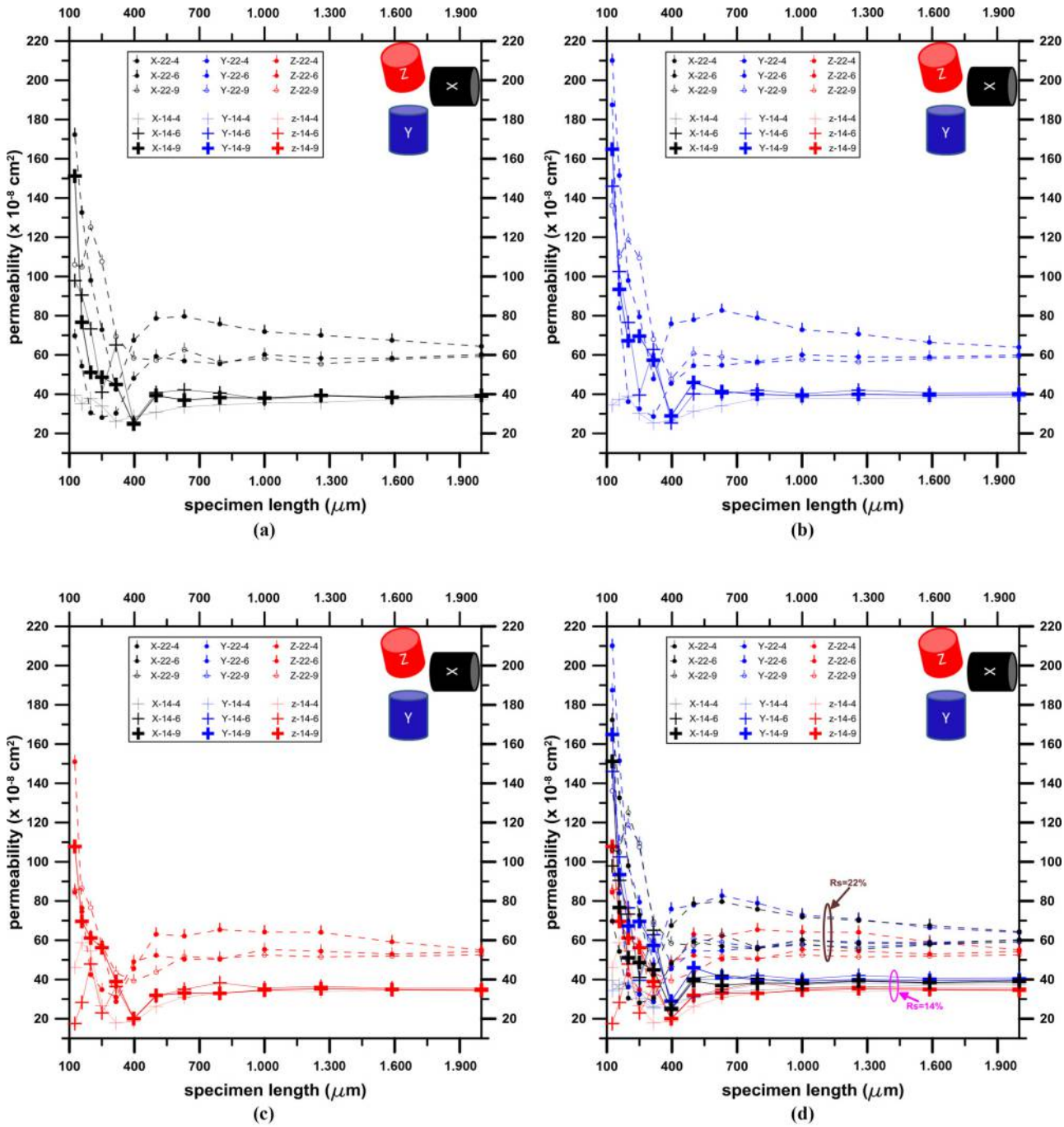

Notes: Results are shown in the (a) x, (b) y and (c) z directions for each of the six samples as well as (d) combined

altered gas permeability. Therefore, there is a vital need for a suitable non-destructive method for:

- permeabilty measurement; and
- correlation to the curing temperature.

The first issue is addressed herein by using CT to provide insight into the spatial distribution of the density of 3D sand moulds under industrial conditions for the 3D printed sand specimens. This would allow the design engineer to simulate the casting process and the solidification of the alloy to be cast in the 3D printed mould even after a long-term storage or delayed transport to another location. The second issue needs to be studied in the future.

The compaction of the sand particles and the special distribution of the furan droplets along each plan, XY, YX and ZX are different due to the machine settings, *eg.* Xr and Rs.

Table II Permeability of the printed specimens, for different speed of the recoater, are compared with the calculated values

Position in the job-box	Re-coater speed (ms^{-1})	Mass (kg)	% of the theoretical density	Density ($kg.m^{-3}$)	Pore volume (%)	Permeability (AFS number)[a]	Minimum Permeability[b] ($\times 10^{-6} cm^2$)		
						Z	X	Y	Z
Z4	0.182	0.13	51	1,345	48	85	36	38	34
Z6	0.182	0.13	51	1,326	49	86	37	40	36
Z9	0.182	0.14	52	1,377	49	77	38	39	35
Z4	0.286	0.13	49	1,301	53	102	58	59	53
Z6	0.286	0.12	48	1,271	53	125	64	64	55
Z9	0.286	0.12	46	1,222	53	130	55	56	52

Notes: [a]Measured, no unit; [b]simulated, on a sample of side length greater than 700 μm

Figure 6 (a), (b) and (c) Backscattered electron images showing the compacted sand particles and furan resin (dark) on them (3D printed sand specimen, Rs = 0.286 ms^{-1} or 22%)

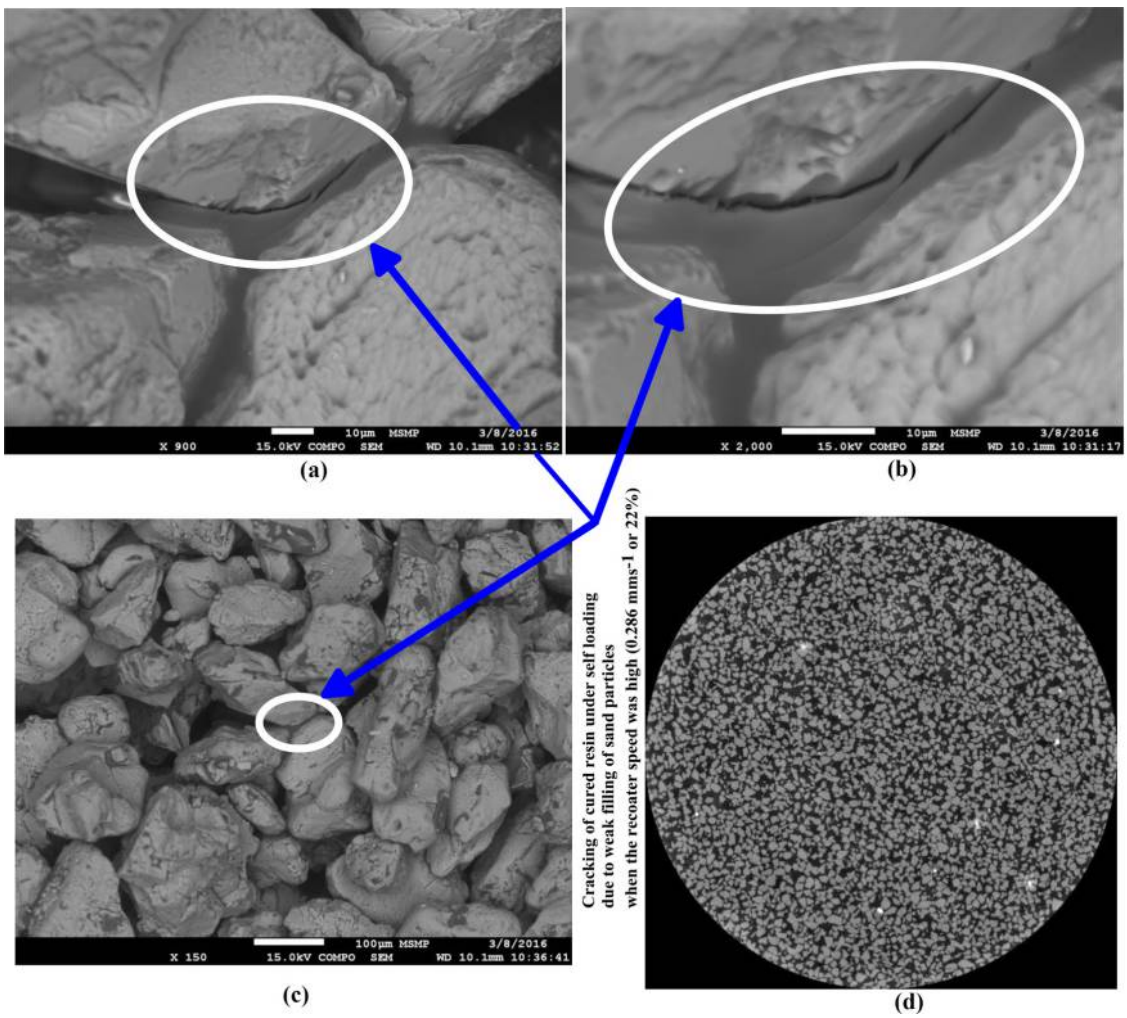

The number of furan droplets per unit area perpendicular to the gas flow direction should influence both permeability and 3PB strength results. Table III shows that the Z-oriented specimen has the highest droplet density in the XY plane and hence this is expected to show very weak gas permeability values of the experimental and simulation results confirm this trend; X- and Y-oriented specimens show similar permeability, and Z-oriented is lower than the others (Figures 3-5). This trend is evident when comparing either Xr (X resolution of the furan droplets) = 120 or 140 μm separately. Both Xr = 120 and 140 μm should show lower permeability in the Z direction when considering the furan droplet area density perpendicular to the gas flow direction. But, the Rs value also influences on the permeability due to non-uniform packing at higher speed

Figure 7 Reconstructed pore model, with the side length of 1000 μm, of the 3D printed sand specimen at locations (top to bottom) Z4, Z6 and Z9 of the job box (Figure 1) with (left) Rs = 14% and (right) Rs = 22%

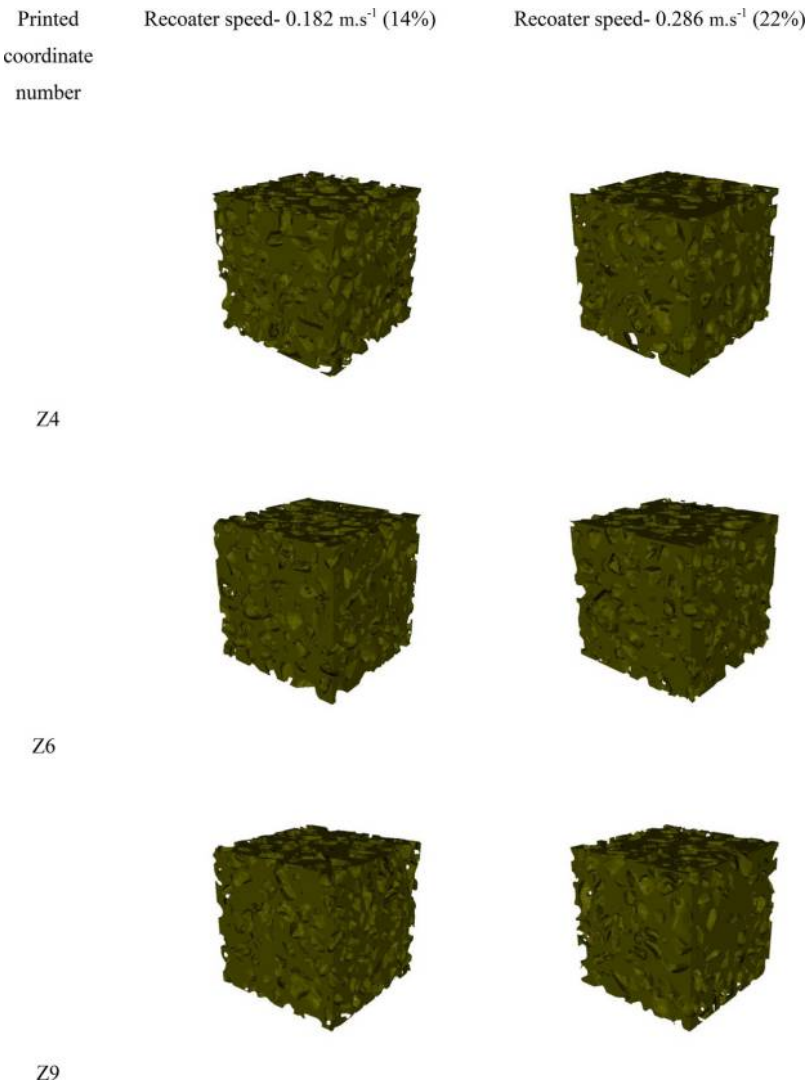

Figure 8 The special distribution of furan droplets perpendicular to X, Y, and Z directions, (the YZ, XZ, and XY planes, respectively)

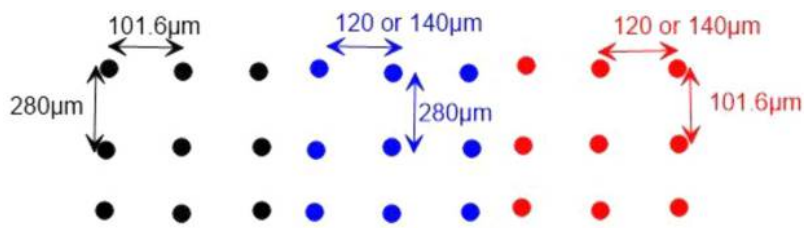

Note: The gas flow direction is perpendicular to this plane during permeability test

than the critical minimum for optimum packing. The Xr value may have an influence on the test results depending on whether it is less than or higher than the average sand grain size. When the furan droplet resolution is smaller than the size of sand grain, the furan droplets may bond all of the sand grains. In the other case, there might be missing furan droplets between the sand grains and causing weaker permeability.

The regions of incomplete packing/bonding can form high volumes of pores if the recoating process is faster than the required minimum; the amount of sand particles supplied is not enough to

Table III Number of furan droplets in each plane per unit area. See also Figure 8

Plane	Furan droplets/area (millions.m^{-2}) When Xr = 120 μm	When Xr = 140 μm
XZ (perpendicular to Y)	29.76	25.51
YZ (perpendicular to X)	35.15	35.15
XY (perpendicular to Z)	82.02	70.30

fill the gap volume created by lowering the job box surface in each iteration during printing. Consequently, the specimen shows lower 3PB strength than the maximum achievable 3PB strength, as well as higher permeability. The high-speed packing also increases the pore connectivity; this might be good for permeability. On the other hand, it causes lower 3PB strength.

A 50 mm specimen printed at the different coordinate of a job box may not be representative of the entire volume of a 3D-printed mould assembly or when considering permeability of a thinner 3D printed sand mould specimen. Usually, a 50-mm specimen is printed along with the parts of the mould assembly and tested assuming the same permeability over the entire volume of the mould assembly. (Sivarupan *et al.*, 2017) stated that the 3D-printed mould assembly would have anisotropic properties due to the variation of furan droplet resolution in all three directions, as this alters the number density of bonded sand particles with the recoater speed. 3D X-ray CT can be used to obtain the permeability of any section on a large mould assembly, which may be the most representative. In this case, a range of permeability values can be obtained to implement the most suitable values for the solidification and filling simulation before casting to predict any solidification issues or even after casting to study the effect of binder content and the thermal degradation behaviour of the furan on casting. The permeability simulation on the model constructed using the 3D X-ray tomography images will be dependent on factors such as the grain size, structural dimensions and geometry, X-ray attenuation coefficients of the materials themselves, as well as the capabilities of the system being used. While it is possible to image large components, there are often practical trade-offs regarding the resolution that can be achieved, the time available to perform the scanning, the field of view that can be captured at a specific resolution, and the influences of various scan artefacts, etc. As such, there will be issues if the same approach is applied to larger scale components – however, the method may be applied to more complex geometry, small-scale parts.

Conclusions

The influence of printing parameters, especially the re-coater speed, on the pore connectivity of the 3D printed sand mould and related permeability has been identified. Characterisation of these sand moulds using X-ray CT and its suitability, compared to the traditional means, are also studied. While density and 3PB strength are a measure of the quality of the moulds, the pore connectivity from the tomographic images precisely relates to the permeability. The main conclusions of the present study are provided below.

- A minimum required sample size of 700 × 700 × 700 μm^3 is required to provide representative permeability results. This was obtained from sand specimens with an average sand grain size of 140 μm, using the tomographic volume images to define a 3D mesh to run permeability calculations.
- Z-direction permeability is always lower than that in the X-/Y- directions due to the lower values of X-(120/140 μm) and Y-(101.6 μm) resolutions of the furan droplets.
- The anisotropic permeability of the 3D printed sand mould is mainly due to, the only adjustable, X-directional resolution of the furan droplets; the Y-directional resolution is a fixed distance, 102.6 μm, between the printhead nozzles and the Z-directional one is usually, 280 μm, twice the size of an average sand grain.
- A non-destructive and most representative permeability value can be obtained, using the computer simulation, on the reconstructed 3D X-ray tomography images obtained on a specific location of a 3D printed sand mould. This saves time and effort on printing a separate specimen for the traditional test which may not be the most representative to the printed mould.

Notes

1 Average particle size 140 μm.

2 Furfuryl alcohol, room temperature density *1130 kg.m^{-3}*.

3 Sulfonic acid, room temperature density *1220 kg.m^{-3}*.

4 Dimensions; radius 50 mm and height 50 mm.

5 Dimensions 22.4 × 22.4 × 172 mm^3.

6 See the discussion.

7 Table 1.

8 Model XT H225 L (Nikon Metrology, UK).

9 The method is explained in a previous publication and briefly in equation 1.

10 This is commonly used in foundries as a unit for gas permeability of sand moulds, but, is not an SI unit.

11 Averaged values of these permeability for greater than the specimen size of 700 × 700 × 700 μm^3.

12 Commercial nomenclature by ExOne^{TM}, FS0001, density 1320-1370 kg.m^{-3}.

13 average particle size 140 μm.

14 Commercial nomenclature by ExOne^{TM}, FS0001, average particle size 140 μm.

References

Coniglio, N., Sivarupan, T. and El Mansori, M. (2018), "Investigation of process parameter effect on anisotropic properties of 3D printed sand molds", *The International Journal of Advanced Manufacturing Technology*, Vol. 94 Nos 5/8, pp. 2175-2185, available at: https://doi.org/10.1007/s00170-017-0861-5

ExOne (2015), "ExOne S-print 3D sand mold printer [WWW document]", *ExOne*, available at: www.exone.com/Systems/Prototyping-Printers/S-Print

Frascati, J.W. (2007), "Effects of position, orientation, and infiltrating material on three dimensional printing models", Electronic Theses and Dissertations, available at: http://stars.library.ucf.edu/etd/3162

Hornung, U. and Springerlink (1997), "Homogenization and porous media", *Interdisciplinary Applied Mathematics*, Springer, New York, NY, Vol. 6, doi: 10.1007/978-1-4612-1920-0.

Jasak, H., Jemcov, A. and Tukovic, Z. (2007), "OpenFOAM: a C ++ library for complex physics simulations", *Int. Work. Coupled Methods Numer. Dyn. m*, pp. 1-20.

Mckenna, N., Singamneni, S., Diegel, O., Singh, D., Neitzert, T., George, J.S., Choudhury, A.R. and Yarlagadda, P. (2008), "Direct metal casting through 3D printing: a critical analysis of the mould characteristics", *9th Glob. Congr. Manuf. Manag.*, pp. 12-14, available at: https://eprints.qut.edu.au/18211/1/18211.pdf

Mitra, S., Rodríguez de Castro, A. and El Mansori, M. (2018), "The effect of ageing process on three-point bending strength and permeability of 3D printed sand molds", *The International Journal of Advanced Manufacturing Technology*, Vol. 97, available at: https://doi.org/10.1007/s00170-018-2024-8

Pavliotis, G.A. and Stuart, A.M. (2008), "Multiscale methods: averaging and homogenization", *Springer Science & Business Media*, Vol. 53, doi: 10.1007/978-0-387-73829-1.

Sivarupan, T., ElMansori, M. and Coniglio, N. (2017), "3D printing process parameters and properties of additively manufactured sand mold for rapid casting: strength and permeability", *Additive Manufacturing (under Review)*.

Upadhyay, M., Sivarupan, T. and El Mansori, M. (2017), "3D printing for rapid sand Casting – a review", *Journal of Manufacturing Processes*, Vol. 29 (October), pp. 211-220, available at: https://doi.org/10.1016/j.jmapro.2017.07.017

Appendix

Figure A1 Permeability of the 3D printed specimen as a function of job-box coordinate and process parameters; for re-coater speed between 10 and 22%, (left) Xr = 0.12 mm (right) Xr = 0.14 mm and for X, Y, and Z orientation as indicated. See colour code in Figure A2 (Sivarupan *et al.*, 2017)

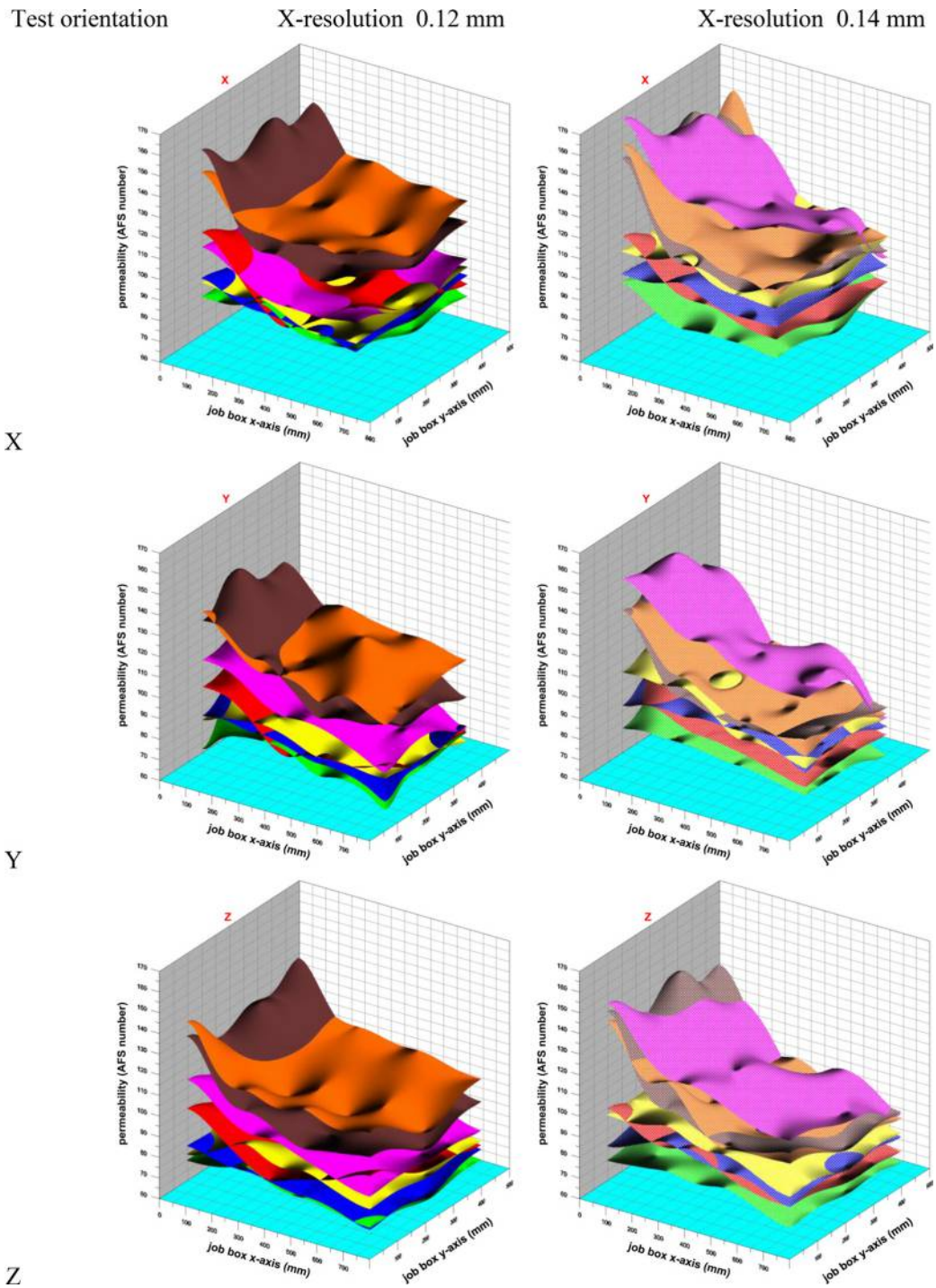

Figure A2 The process parameters used in the experiments. Sand particle size (140 μm), activator content (0.18 Wt.% of sand), mixing time of sand[14] and activator (60s), magnesium inhibitor (0.4 Wt.% of sand), heating temperature (32°C) and print head voltage (78V) were all kept constant (Sivarupan *et al.*, 2017)

Sand re-coater speed (R_s)		X or Y-resolution of furan droplets (X_r/ Y_r)	Colour codes used in Fig. A-1
(% of max. speed)	(ms^{-1})	(mm)	
10	0.130	0.12	
10	0.130	0.14	
12	0.156	0.12	
12	0.156	0.14	
14	**0.182**	**0.12**	
14	0.182	0.14	
16	0.208	0.12	
16	0.208	0.14	
18	0.234	0.12	
18	0.234	0.14	
20	0.260	0.12	
20	0.260	0.14	
22	0.286	0.12	
22	**0.286**	**0.14**	

Corresponding author

Tharmalingam Sivarupan can be contacted at: t.sivarupan@uq.edu.au